Effect of Solvent Additives and P3HT on PDTSTTz/PCBM Based Bulk Heterojunction Solar Cells

Asegid Ergete

A Thesis Submitted to Materials Science Program Presented in Partial Fulfillment of the Requirements for the Degree of Master of Science in Materials Science

Addis Ababa University

Addis Ababa, Ethiopia

May, 2013

Addis Ababa University

School of Graduate Studies

This is to certify that the thesis prepared by Asegid Ergete, entitled: Effect of *Solvent Additives and P3HT on PDTSTTz/PCBM Based Bulk Heterojunction Solar Cells;* and submitted in partial fulfilment of the requirements for the degree of Master of Science in Materials Science complies with the regulations of the University and meets the accepted standards with respect to originality and quality.

Signed by the Examining Committee:

Examiner: Dr. Siraye Esubalew Sign. _____ Date 04/07/2013

Examiner: Prof. Javed Mazher Sign. _____ Date 04/07/2013

Advisor: Prof. Teketel Yohannes Sign. _____ Date 04/07/2013

_____

Chair of Department or Graduate Program Coordinator

Abstract

Effect of Solvent Additives and P3HT on PDTSTTz/PCBM Based Bulk Heterojunction Solar cells

Asegid Ergete

Addis Ababa University, 2013

The dependency of the performance of organic bulk heterojuction (BHJ) solar cells on the nanomorphology of the photoactive blend can be controlled by solvent additives. In this work BHJ solar cells based on PDTSTTz:PCBM (1:1) which processed by using a host solvent di-chlorobenzene and 2.5% (v/v) different solvent additives such as iodobutane, iodoethane, di-iodomethane, and iodomethane were constructed. The effects of the aforementioned additives on the photovoltaic parameters of the solar cells were investigated. Devices processed in 2.5% (v/v) of iodobutane exhibited the highest power conversion efficiency (PCE) up to 2.02% as compared to the pristine PDTSTTz:PCBM devices (without additive) (0.39%). The UV-Vis absorption spectra of films showed the existence of red shift in the presence of these additives resulting from the growth of enhanced local structure with distinct, optimized phase separated morphology. Besides, the introduction of P3HT donor into PDTSTTz/PCBM system forming a ternary blend also showed improved efficiency (2.42%) following the increased short circuit current up to 11.08 mA/cm^2 through improved photon harvesting.

KEYWORDS - Organic Solar Cell, Additive, Morphology, Bulk Heterojunction

Acknowledgements

My heartfelt gratitude is to my advisor, Prof. Teketel Yohannes, thank you for accepting me into your group for my Final Thesis Work. It has been a fruitfully challenging experience, and doing this thesis under your group has shown me again the importance of deep thinking skills. Thank you again for your enthusiastic approach and guidance in all my work.

To my mentor, Fedilu Kedir, Ph.D. candidate, for being kind and patient while always guiding me when I need help. Thanks for all the time spent teaching me and all-round mentoring even though you are also constantly busy. It has been a great joy and pleasure meeting you, making this Thesis Work a lot more fun.

To Dr. Getachew Adam, Dilla Univesity; Bekele Hailegnaw, Bahir Dar University; Newaye Medihin, Ph.D. candidate; thank you for you are really helpful to support and share your experiences. To Prof. Javed Mazher, thank you a lot. You have been responsibly and constantly asking me on my continuities for my best during this Thesis Work; and your constructive comments were inputs for my work to be complete. My exceptional gratitude also goes to Dr. Siraye Esubalew, I learnt a lot from your comments; not only for this work but also for the rest of my life. To materials Science Secretary, I thank you. I like the way you approach and treat students. To all other members and colleagues, many thanks for any assistance that all of you have provided. It is great to have known such nice and friendly people. Especially, Behailu Mamo, I thank you for all you did for me.

To Prof. Young Fang Li along with his research group; Institute of Chemistry, Chinese Academy of Sciences, Beijing, China, for his willingness to provide the polymer which I have used for my work.

Then, I would like to thank Addis Ababa University, Department of Chemistry, Physical Laboratory; Materials Science Program, for the unlimited support to my work from inception to completion. Finally, to the Ethiopian Ministry of Mines, for allowing me to join the graduate study.

Table of Contents

List of Figures

List of Tables

List of Abbreviations

BHJ	Bulk Hetrojunction
DCB	Dichlorobenzene
DHPT3	ethieno[3,2-b]thiophene-alt-pentathiophene
DIMe	di-iodomethane
EQE	External Quantum Efficiency
FF	Fill Factor
HOMO	Highest Occupied Molecular Orbital
I_{sc}	Short circuit current
IBu	iodobutane
IEt	iodoethane
IMe	iodomethane
IPCE	Incident Photon-to-Current Conversion Efficiency
ITO	Indium Tin Oxide
J_{sc}	Short circuit current density
LUMO	Lowest Unoccupied Molecular Orbital
MEH-PPV	Poly(2-methoxy-5-(2-ethylhexyloxy)-1,4-phenylenevinylene
MPP	Maximum Power Point
OPV	Organic Photovoltaics
PCBM	[6,6]-phenyl-C61-butyric acid methyl ester
PCE,	Power Conversion Efficiency

PDTSTTz	poly[2,6-(4,4'-bis(2-ethylhexyl)dithieno [3,2-b:2',3'-d]silole)-alt-5,5'-(3,6-bis[4-(2-ethylhexyl)thienyl-2-yl]-s-tetrazine)]
PEDOT:PSS	*Poly*(3,4-ethylenedioxythiophene): Ppoly(styrenesulfonate)
PPV	Poly(P-phenylenevinylene)
P3HT	Poly-3-hexylthiophene
UV-Vis	Ultraviolet Visible
V_{oc}	Open circuit voltage

1. Introduction

The modern world is highly energy dependent and demanding increases in the energy supply. The increase in the energy demand is due to industrialization, urbanization and increasing population. Without energy, no development; and hence, the availability of energy resources will mainly determine any country's economy and standards of living. The finite supply of traditional fossil fuels (oil, natural gas, coal, etc.) underlines the need to look for alternative energy sources. It is estimated that in another 200 - 300 years [1], fossil fuels will be depleted resulting in a devastating situation. Besides, the usage of fossil fuels is related to environmental issues such as climate change and global warming. Therefore, a sustainable, environment friendly renewable energy source is needed. Renewable energy resources like solar energy (direct conversion of sun light into energy), hydro, biomass, wind, etc., are particularly attractive.

Solar energy is one of the promising renewable energy sources because it is inexhaustible and pollution free. Solar energy is converted into electricity by means of solar cells. Effective use of this energy can mitigate future energy needs. Methods of solar energy utilization can be broadly classified into two categories (i) photothermal and (ii) photovoltaic. Photothermal systems convert solar radiation into thermal energy which can be used directly. Photovoltaic systems (solar cells) convert sun light into direct electricity. Traditional solar cells are mainly based on inorganic semiconducting materials, crystalline and amorphous silicon. However, silicon solar cells are not widely used thus far. The reason is that silicon photovoltaic technology is very complex, resulting in high cost of silicon solar cells.

Organic solar cells are being extensively studied worldwide since they have the potential to inexpensively produce electricity from solar energy. The flexibility is another important advantage of organic solar cells. Methods for the fabrication of organic layers of organic solar cells may include spin-coating, drop casting, vapor phase deposition, etc. In our work, spin-coating technique was used for many of its advantages. The possibility to form uniform thin films, cheap, fast and simple to operate; are some of the benefits of spin-coating technique.

1.1. Historical Background of Organic Photovoltaics (OPVs)

The single layer device structure of OPV cells was created in 1994 by R. N. Marks *et al.* [1] using 50 - 320 nm thickness of *poly*(p-phenylenevinylene) (PPV) sandwiched between a high work function transparent ITO (better alignment with HOMO of donor) and a low work function cathode (better alignment with LUMO of the acceptor). The reported quantum efficiencies for this device were around 0.1%.

This low quantum efficiency resulted from intrinsically low mobility of charges through semiconducting organic materials. The carrier mobility of semiconducting organics remains around 10^{-3} cm^2/Vs, while the mobility of single crystalline silicon is about 10^3 cm^2/Vs order. This indicates that the photogenerated charges in semiconducting organics require more time to be collected from electrodes. The slow charge transport itself not only lowers the efficiency of the OPV cell, but also increases the recombination chance of charges in the device. The other problem that causes the low PCE of OPV cells is exciton formation. Photogeneration in organic semiconductors does not directly lead to free charge carriers; instead columbically

bound electron - hole pairs of photoexcited states are formed [2]. Free electrons and holes are desired as an efficient charge carrier because the bound exciton requires an additional exciton dissociation step to make free carriers, which can decrease the carrier generation efficiency. In a single layer OPV cell, the only exciton dissociation site (into free electrons and holes) is the interface between semiconducting organics and a cathode. Later, it was known that the excitons are more efficiently dissociated at the interface between donor and acceptor, and a bilayer OPV cell was developed by inserting an acceptor layer between a donor semiconducting organic and a cathode.

The bilayer OPV cell structure includes an additional electron transporting layer than the single layer OPV structure. This structure was first realized by C. W. Tang in 1985 [3] with a device structure comprising indium tin oxide (ITO)/copper phthalocyanine (CuPc)/ perylene tetracarboxylic derivative (PV)/silver (Ag). The reported PCE was reached up to 1%. The ten-fold PCE increase, than the single layer, resulted from improvement in the exciton dissociation efficiency *via* the acceptor material that forms an offset energy band with hole transporting material. However, the reported PCE of bilayer OPV cells is still significantly lower than that of inorganic based PV cells. One reason for this is the intrinsically short exciton diffusion length of excitons in organic semiconductors, which are typically around 10 – 20 nm [4 - 7]. Sariciftci *et al.* [8] fabricated the first bilayer OPV cell that used a conjugated polymer where the hole transporting material was MEH-PPV and the electron transporting material was fullerene, C_{60}. In this OPV cell, the observed PCE was 0.04% under monochromatic incident light at 514.5 nm, and the performance was only slightly improved compared to single polymer layer PV cells. Halls *et al.*[9]

optimized the thickness of conjugated polymer and C_{60} layer and achieved 9% quantum efficiency.

After discovering the conjugated polymer blend OPV cell, Yu *et al.*[10] also reported improved PCE from the conjugated polymer and C_{60}-based bulk heterojunction OPV cell. Composite films of MEH-PPV, and fullerenes exhibited PCE of about 2.9%, which is better by more than two orders of magnitude than what has been achieved with devices made with pure MEH-PPV. The efficient charge separation results from photoinduced electron transfer from MEH-PPV (as donor) to C_{60} (as acceptor) at the large interfacial contact as a result of mixing, and the high collection efficiency results from a bicontinuous network of internal donor acceptor heterojunctions.

Nowadays, organic solar cells based on bulk heterojunction (BHJ) structure consisting of conjugated polymers as electron donors and fullerene derivatives as electron acceptors are considered as the promising; and their efficiency exceeded 9% [11, 12] using various treatments such as thermal annealing, using solvent mixtures, solvent additives, etc. Addition of a 2 – 3% (v/v) solvent additive during the processing of the active layer is the most effective means of optimizing a BHJ device's morphology [12]. It selectively dissolves one component of the photoactive blend and enhances the self organization of the polymer units into ordered crystalline structure thereby increasing the nano-scale donor-acceptor interface contact area to reduce the interfacial power losses due to recombination of holes and electrons.

The subject of this work focuses on the construction and characterization of solution processable BHJ organic solar cells, based on PDTSTTz/PCBM donor-acceptor

system. The respective effects of addition of solvent additives and a second electron donor, P3HT, to PDTSTTz/PCBM system will be investigated. Here we anticipate that solvent additives will affect the film morphology; and P3HT to increase the absorption coverage.

PDTSTTz is a low band gap polymer with broad absorption in the longer wavelength range (desirable for harvesting low energy photons); and low lying highest occupied molecular orbital, HOMO, level (for extended open circuit voltage), capable of maximizing the overall power conversion efficiency (PCE). The detailed procedure and synthesis route for PDTSTTz is in the reported literature [13]. Solar cells from the blend of this polymer with $PC_{70}BM$ showed power conversion efficiency (PCE) up to 5.59% [13] in an inert atmosphere and using various treatments. Here, PDTSTTz is blended with $PC_{61}BM$ (or PCBM) acceptor with a sole objective of studying the effect of short chain iodoalkane solvent additives (for their selective solubility to fullerene) on the photovoltaic parameters, and the dependency of device performance on alkyl chain length. The performance of PDTSTTz, when combined with other compatible donor (like P3HT) as a ternary system, is also investigated.

2. Literature Review

2.1. Electronically Conducting Polymers

Because of their light weight, flexibility and the greater ease of fabrication, polymers are continuing to replace metals in several areas of applications; as often remarked 'from buckets to rockets'. Polymers have traditionally been treated as good electrical insulators and a variety of their applications have relied on this insulating property.

However, there are some polymers which become electrically conducting when treated with strong oxidizing or reducing agents. The chemical structure of some common polymers is shown in Figure 1. A common characteristic of all of them is the existence of conjugated bonds (extended π-conjugation along the polymer backbone) [14].

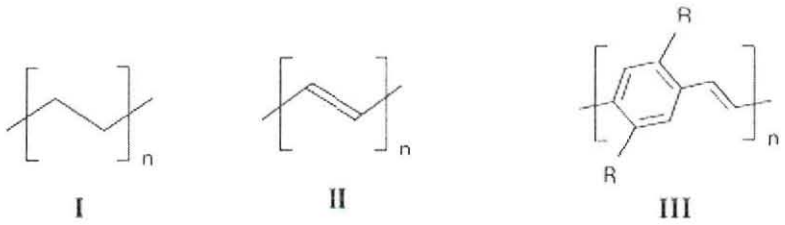

Figure 1. Chemical structure of some common polymers. (I) polyethylene, or PE; (II) *trans*-polyacetylene, or PA; (III) poly(*para*-phenylenevinylene), or PPV.

2.1.1. The Origin of Semiconducting Behaviour

Since carbon atom (C-atom) is the main building block of most organic polymers, the type of bonds that its valence electrons make with other C-atoms or other elements determine the overall electronic properties of the respective polymer. Polymers can be saturated and unsaturated. Saturated polymers are insulators since all the four valence electrons of C-atom are used up in covalent bonds; whereas unsaturated polymers have conjugated structure and they are conductive. π-conjugated polymers are excellent examples of unsaturated polymers alternate single and double carbon-carbon bonds.

The fundamental source of semiconducting property of conjugated polymers stems from the overlap of the molecular orbitals formed by the valence electrons of chemically bonded C-atoms. Every carbon atom has four valence electrons in which two valence electrons are in the 2s orbital and the other two in two different 2p orbitals in its ground state. A conjugated polymer chain possesses sp^2 hybridized orbitals. As shown in Figure 2, the overlapping of these orbitals results in sigma bond. The remaining, the fourth valence electron is positioned in a 2p orbital that is perpendicular to the plane formed by the three sp^2 orbitals. Each electron in the 2p orbital along the chain interacts with a neighbouring 2p electron and forms a π-bond. The two electrons in a π-bond occupy the space above and below the σ- bond [15].

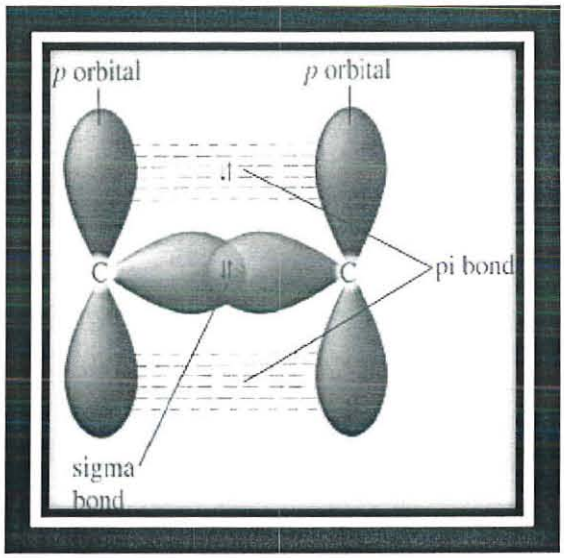

Figure 2. Illustration of σ- and π- bonds between two carbon atoms [15].

In analogous to the inorganic semiconductors, a polymer unit cell interacts with its neighbours resulting in the merging of discrete sets of molecular electronic states to form electronic bands. These bands are referred as valence band (VB) corresponds to

the highest occupied molecular orbital (HOMO); and the conduction band (CB) corresponds to the lowest unoccupied molecular orbital (LUMO).

For instance, polyacetylene, the simplest conjugated polymer, formed from the repeating units of ethylene units. As the conjugation chain length increases from left to right (see Figure 3), the molecular orbitals progressively develop into a band structure and the separation between HOMO and LUMO decrease to develop a band. For shorter polyene chains, Δ represents the HOMO-LUMO energy gap (E_g). For the infinite polyene chains, VB and CB represent the valence band and the conduction band respectively and E_g is the energy bandgap [16].

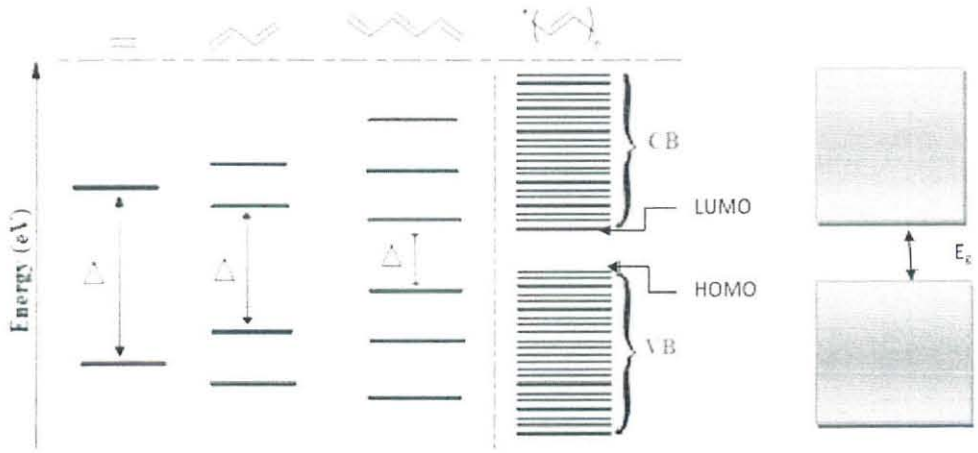

Figure 3. The development of a polyacetylene band structure from the molecular orbitals of ethylene.

As the ethylene units are united and form a larger molecule (shown in Figure 3), the π-bonding will become more delocalized, and more atomic orbitals are involved in the overall molecular orbital system. When two ethylene molecules coupled to form 1,3-

butadiene. The HOMO-LUMO gap of butadiene is slightly smaller than that of ethylene monomer. This reduced gap is due to the increase in conjugation in this π-system relative to that of ethylene. Generally as adding ethylene units is continued, longer conjugated systems will be created. An infinite one-dimensional polyene chain containing infinite number of bonding and antibonding molecular orbitals has been formed. In this infinite chain, the bonding orbitals will tend to cluster together into a tightly bound group, and the antibonding orbitals will tend to cluster into another tightly bound group. The two groups are well separated producing a well defined HOMO-LUMO energy gap. Each of the molecular orbital distributions consists of a large number of orbitals that are packed tightly together into a finite energy interval. For most purposes, we can ignore the difference in their energy interval as the orbitals form continuous bands of energy levels. The cluster of fully occupied π-bonding orbitals is referred to as the valence band (VB) and the cluster of vacant antibonding orbitals is called the conduction band (CB). Under this condition, the HOMO-LUMO gap is called the bandgap (E_g). This gap determines the optical properties and is a characteristic of a given polymer.

2.1.2. Charge Carriers in Conducting Polymers

The presence of mobile charge carriers is compulsory for charge transport in any material. Unlike inorganic semiconductors, the charge carriers in conducting polymers are not free electrons or holes; instead they are quasi-particles. The three types of quasi-particles in conducting polymers are solitons, polarons and bipolarons.

i. Solitons: are defects of a conjugated polymer formed as a result of mis-fit combination of energetically degenerate structures.

ii. Polarons: are combination of charge and the surrounding deformation formed by the combination of non-degenerate ground state isomers of conducting polymers that leads to the formation of structural defect (misfit).

iii. Bipolarons: combinations of two plarons.

2.2. Photovoltaics (PVs)

A photovoltaic cell or solar cell is a device that can convert light energy into electricity directly. Becquerel first discovered the photovoltaic effect by placing two electrodes in an electrolyte solution in 1839 [17]. Silicon based solar cells recently achieved 24% efficiency approaching theoretical limit of 30% [18, 19]. However, high production cost of these inorganic solar cells, mainly attributed to processing at high temperatures (400 - 1400^{O}C) and the involvement of expensive vacuum capital equipment, is the reason for slow adoption into the terrestrial market.

2.2.1. Organic Photovoltaics (OPVs)

Organic photovoltaics can be a potential candidate for developing low cost power generation that is economically practicable for large scale applications. Compared to traditional Si based solar cells, organic materials are less expensive. Easy processing through spin coating or dip coating techniques is an added advantage, eliminating the costly vacuum processing conditions. High absorption coefficients compared to Si, the use of very thin films, 10 -50 times thinner than Si based devices, is possible [20]. Thin films facilitate the possibility of producing thin flexible devices with high throughput. In organic solar cells technology, there are many concepts based on small

molecules, conjugated polymers, conjugated polymer blends, bi-layer devices based on small molecules and conjugated polymers. A widely used concept in organic solar cells is the use of polymer/fullerene blends.

2.2.2. Architecture of Organic Photovoltaic Devices

The structure of a typical polymeric photovoltaic device consists of the photoactive layer usually sandwiched between indium tin oxide (ITO) coated substrate (glass or plastic) electrode and reflective back metal electrode (usually Aluminium). The two electrodes can be further modified to improve the charge injection by the introduction of a PEDOT:PSS (*poly*[3,4-ethylenedioxythiophene]:*poly*(styrene sulfonate)) as a hole transporting layer to be coated on the ITO side and lithium fluoride (LiF) layer deposited under layer on the aluminium side. The optimum thickness of photoactive layer in most polymer solar cells is ~100 nm [21]. Active layer thickness very higher than this optimum value will increase the series resistance and the short circuit current (I_{sc}) breaks down because of the low mobility of polymeric semiconductors charge carriers typically as low as ~ 10^{-4} $cm^2/V.s$ [22]. Such thin layers have, of course, limited absorption even at the peak of their absorption spectrum. But because of the very high optical absorption coefficients of polymers (> 10^5 cm^{-1}) [23], this thin layer (~ 100 nm) can absorb enough photons to yield high photocurrent [24, 25]. The device architecture of the photoactive layer has a strong impact on charge carrier separation and transport. Figure 4 represents a schematic device structure for a typical organic solar cell.

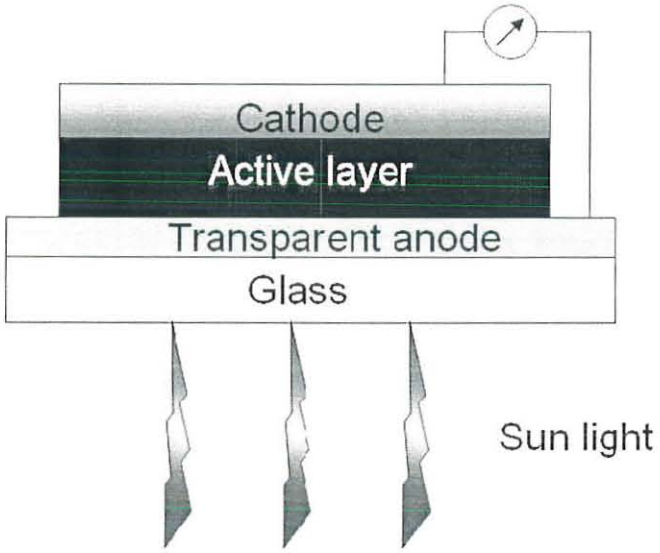

Figure 4. Schematic layout of a typical organic solar cell.

For better power conversion efficiency, many attempts had been made by scholars of the field to get photovoltaic devices with different layered structures as described next.

2.2.2.1. Single Layered Organic PV Cells

It is the simplest device structure in which a single organic material is sandwiched between two different conducting contacts, typically indium tin oxide, ITO, and a low work function metal such as Al, Ca or Mg. Although these cells tend to produce a reasonable open circuit voltage (V_{oc}), their photocurrent is typically very low. This is mainly due to the recombination of photogenerated electrons and holes, and the maximum efficiency reported with this architecture is 1% [26, 27]. Charge carriers

can only be dissociated at the schottky junction. Therefore, only excitons generated close to the electrode can contribute to the photocurrent.

2.2.2.2. Bilayer Organic PV cells

This design contains the donor–acceptor system, in which the exciton is dissociated at their interface, where the holes transfer to the donor and the electrons to the acceptor. Thus, the different types of charge carriers may travel independently within separate materials and bimolecular recombination is highly minimized [28]. However, the short diffusion length of excitons still limited the power conversion efficiency to be low.

2.2.2.3. Bulk Heterojunction (BHJ) Organic PV Cells

The problem of poor exciton collection (or low J_{sc}) was later solved by the bulk heterojunction (BHJ) structure [11], where the donor-acceptor interface is distributed randomly throughout the volume of the cell. Thus, excitons can efficiently be harvested regardless of the point of photo-excitation leading to high J_{sc}. Unfortunately, this system suffers from higher recombination of the photo-generated carriers at the increased donor/acceptor junction that reduces its open circuit voltage, V_{oc}, and the fill factor (FF).

The bulk heterojunction (BHJ) is the most widely used structure, because it comprises ease of processing, best electron donor-acceptor interface and improved efficiency. It overcomes the limitations of the two layer concept where recombination of the carriers due to long range donor-acceptor (D-A) interfacial length is reduced and high surface area of D-A interface is formed. The large D-A interface surface area reduces

the distance that excitons need to travel to reach the interface, and hence charge separation can take place throughout the whole depth of the photoactive layer [29, 30]. During the preparation of the photoactive layer of BHJ solar cells by mixing the donor and acceptor materials with a nanoscale phase separation, three-dimensional interpenetrating network of electron-donor (D) and electron–acceptor (A) domains will be formed [31]. Currently used electron acceptor materials for BHJ organic solar cells are composites of electron-conducting fullerenes, mostly the derivative of [6,6]-phenyl-C_{61}- butyric acid methyl ester ($PC_{61}BM$) , and hole-conducting conjugated polymers such as poly(3-hexylthiophene), P3HT.

2.2.2.4. Ternary Blend BHJ Organic PV Cells

Ternary blend PV cells can be designed based on two donor components and one acceptor component, or one donor and two acceptors (see Figure 5) have exhibited far less attention; but have been recognized as a potential route to increase the absorption width at half height and consequently the short circuit current density (J_{sc}).

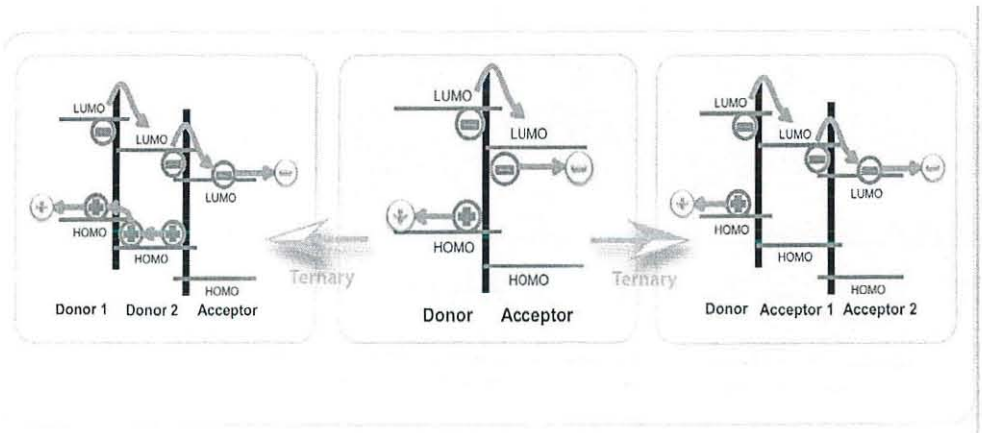

Figure 5. Schematic diagram for the design of BHJ ternary blend organic solar cells.

Ternary blend BHJ solar cells offer an alternative approach for maximizing the attainable $J_{sc}V_{oc}$ product while retaining the simplicity of active-layer processing steps. In many cases, larger J_{sc} is observed relative to the binary systems. Measurements of the photocurrent spectral response and the open-circuit voltage show that the HOMO and LUMO levels change continuously with composition in the respective two component acceptor or donor pair, consistent with the formation of an organic alloy [32]. However, optical absorption of the exciton states retains the individual molecular properties of the two materials across the blend composition. This difference is attributed to the highly localized molecular nature of the exciton and the more delocalized intermolecular nature of electrons and holes that reflect the average composition of the alloy.

2.2.3. Working Principle of BHJ Organic PV cells

The device structure appears similar to the inorganic solar cells; but the operational physics is a bit different. The proper choice for combining materials in organic solar cells should be made based on the energy levels, such as ionization potential (IP) and electron affinity (EA) that will help to determine the possible materials for the desired system. When two different materials with different HOMO, LUMO levels are brought in contact, band bending will occur depending on the relative position of the Fermi levels. This band bending causes charge transfer in the system that will be determined by the HOMO, LUMO levels. This can be well understood when one material has a low EA and another high IP where the low EA material will donate the electron to the conduction band (CB) of the other and the low IP material will accept the hole from valance band (VB) of the other. Energy transfer will occur in the system when a higher bandgap material and a lower bandgap material are present in the

system. This process is termed as Forster transfer [33] where excitation energy transfers to the low bandgap material with small losses.

Creation of charges is one of the key steps for better photovoltaic device performance. In most organic solar cells, charges are created by photo-induced electron transfer. Absorption of the light will create columbically bound electron–hole pairs (called excitons). Breaking these excitons will result in free charges. Exciton dissociation is facilitated by the built-in electric field [34, 35]. The difference in the work functions will create the built-in electric field. Excition dissociation will take place mainly at the interfaces. The operation principle of BHJ organic PV cells involves some consecutive fundamental steps:

i. Exciton Formation *via* Absorption of Photons

First, incident photons with an energy equal to or beyond the band gap of the polymer are absorbed by the donor polymer material and excite the electrons from the highest occupied molecular orbital (HOMO) to the lowest unoccupied molecular orbital (LUMO) level, creating columbically bound excitons (with a certain binding energy, typically 0.2 – 0.5 eV) [14]. The relative dielectric constant of organic polymers is in the order of 2 – 4, as compared to the inorganic semiconductors (i.e. 10) [15], results in such a strongly bound *Frenkel*-like localized excitons which are not affected by the thermal energy of room temperature, k_BT.

ii. Exciton diffusion

After excitons are formed, they diffuse to the donor-acceptor (D-A) interface across the polymer domain in the range of the characteristics diffusion length (L_D) to generate separated free charge carriers. The diffusion length for most conjugated polymer excitons is typically in the range 5 – 20 nm [15]. Since excitons are neutral species that do not respond to any electric field, their motion is relied on diffusion *via* random hoping driven by the concentration gradient within their characteristics diffusion length range. Those excitons that do not reach the D-A interface have no contribution to the photocurrent generation and are lost *via* recombination.

iii. Dissociation of Charge Carriers

After excitons transfer to the donor-acceptor interface, and consequence dissociation, the electrons are localized in the electron acceptor (commonly PCBM) phase whereas the holes remain in the donor polymer chains. Then, the free electrons transported through the acceptor pathway towards the cathode through which they enter into the external circuit to generate electricity up on its motion. Holes return back to the HOMO of the donor and transported towards the counter electrode (anode) for regeneration. These charge carrier transport towards the respective electrodes is driven by an internal electric field driven from the Fermi-level difference of the electrodes with efficiencies depending on their mobility during the hopping process. Such photo-induced charge transfer between electron donor and acceptor is always in competition with recombination and photoluminescence, although these competing processes take large time scale (photoluminescence (ns) and recombination (μs)) as compared to the charge transfer which occurs in the range 50 fs [16]. For better efficiency of a given BHJ solar cell, there should be efficient carriers transport to the

respective electrode with less recombination. This is dependent on the fraction of excitons that reach the D-A interface which is determined by the exciton diffusion length and the location at which an exciton is created with respect to the nearest dissociation center.

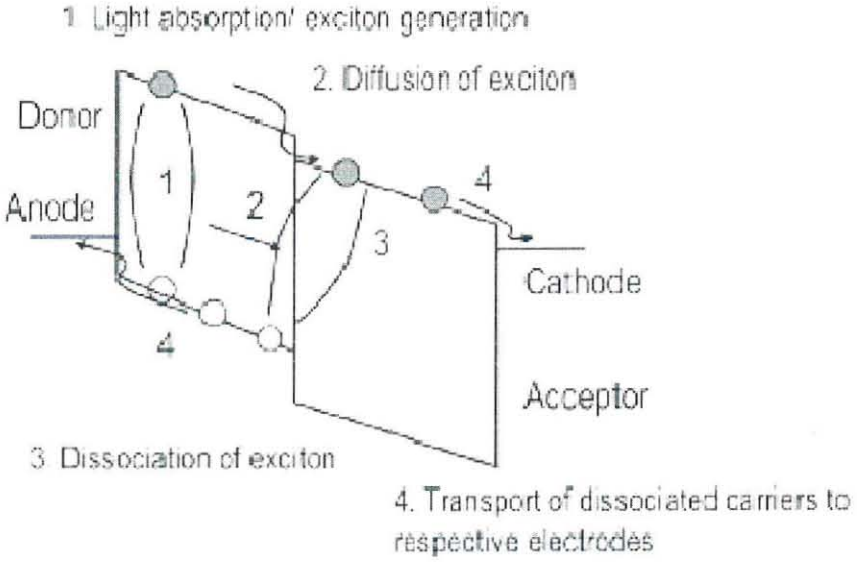

Figure 6. Schematic diagram showing the entire processes for the operation of BHJ organic solar cells.

2.2.4. Criteria for an Efficient BHJ Solar Cell Polymer

A conjugated polymer should possess favorable physical and chemical properties in order to achieve reasonable device efficiency. Key words such as large absorption coefficient, low band gap, high charge mobility, favorable blend morphology, environmental stability, suitable HOMO/LUMO level and high solubility.

2.2.4.1. Large Absorption Coefficient

For an efficient collection of photons, the absorption spectrum of the active layer should align with the solar spectrum. Polymers used in solar cells should have large absorption coefficient in the film state for a successful application since the preliminary physics related to photovoltaic phenomenon is photon absorption. Acceptor materials like, $PC_{60}BM$ or $PC_{70}BM$, absorb inefficiently longer than 400 nm [36]. It is thus the responsibility for the polymer (donor) to harvest low energy photons above 400 nm. The means to increase the solar absorption of the photoactive layer include: 1) increasing the thickness of the photoactive layer; 2) increasing the absorption coefficient; and 3) matching the polymer absorption with the solar spectrum [37]. The first strategy is rather limited due to the fact that the charge-carrier mobility for polymeric semiconductors can be as low as 10^{-4} cm^2/Vs. Increasing the photoactive layer thickness is advantageous for light absorption but burdens the charge transport. This is because the series resistance of the device increases significantly upon increasing the photoactive layer thickness and this makes devices with thick active layer hardly functional. The short-circuit current (J_{sc}) may also drop as well because of the low mobility of charge carriers. With the limitation to further increase the thickness, large absorption coefficient (10^5 to 10^6) in the film state is preferred in order to achieve photocurrent >10 mA/cm^2 [38]. Another option is lowering the bandgap so that the absorption of the polymer can be broadened to longer wavelength and low energy photons ($\lambda > 800$ nm) can be captured as well.

2.2.4.2. Low Bandgap for Long Wavelength Photoabsorption

The solar irradiation spectrum at sea level is shown in Figure 7 [39]. The photon energy is distributed roughly from 300 nm to 1000 nm. However, for a typical conjugated polymer whose energy gap, E_g, is ~ 2.0 eV, only photons of wavelength up to 600 nm can be absorbed (B in Figure 7) with maximum 25% of the total solar energy. Through increasing the absorption onset to 1000 nm (E_g ~ 1.2 eV) (C in Figure 7), approximately 70 to 80% of the solar energy will be covered. An important argument with the low band gap polymer is that once a polymer absorbs at longer wavelength, there will be absorption hollow at the shorter wavelength side, which consequently decreases the incident photon to electron conversion efficiency at that range.

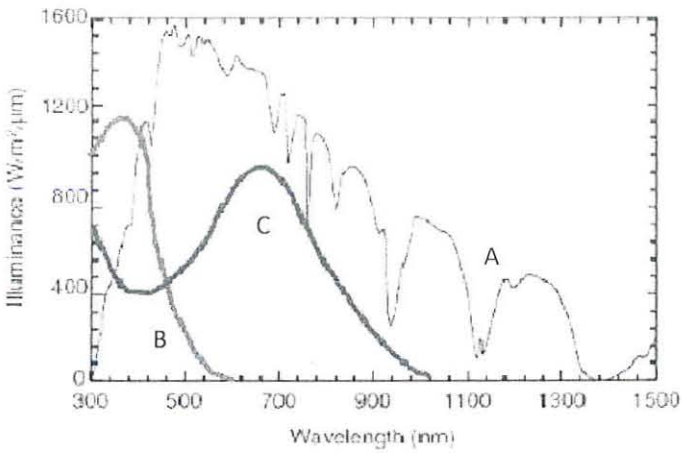

Figure 7. Reference solar irradiation spectrum of AM1.5 illumination (A); typical absorption spectrum of a large band gap polymer (B); and typical absorption spectrum of a narrow band gap polymer (C) [39].

One approach to address this issue is to fabricate a tandem solar cell with both large bandgap polymer and narrow bandgap polymer and used simultaneously for solar

photon harvesting. The other approach is to use ternary blend BHJ solar cells which can offer a distinct platform and an alternative way for increasing the attainable power output while maintaining the simplicity of active layer processing.

2.2.4.3. High charge carrier mobility

Charge transport properties are critical parameters for efficient photovoltaic cells. Higher charge carrier mobility of the polymer increases the diffusion length of electrons and holes generated during photovoltaic process and at the same time reduce the photocurrent loss by recombination in the active layer. This improves the charge transfer efficiency from the polymer donor to the acceptor. This charge transport property of the photoactive layer is the manifestation of the charge transporting behavior of both the donor polymer and the acceptor. For instance, the electron transport property of pure PCBM thin film has been reported in details and is known to be satisfactory for high photovoltaic performance (~10^{-3} cm^2/Vs) [40]. However, the mobility of the free charge carriers in thin polymer films is normally in the order of 10^{-3} to 10^{-11} cm^2/Vs, which limits the PCE of many reported devices [41]. Therefore, it is promising to increase the efficiency by improving the charge carrier property of the polymer part, since there is huge space to improve.

2.2.4.4. Stability

The air stability of the solar cell device has attracted more attention from many research groups. Although industry pays more attention to the cost rather than the durability of the solar cell device, a shelf lifetime of several years as well as a reasonably long operation lifetime are required to compete in the market. The air

instability of solar cell devices is mainly caused by polymer degradation in air, oxidation on low work function electrode, and the degradation of the morphology of the photoactive layer. Oxygen, for its high electron affinity, will oxidize the polymer forming traps to the free charge carriers; and corrode the electrode contact *via* formation an oxide Thus, a conjugated polymer should have intrinsic stability towards oxygen oxidation which requires the HOMO energy level below the air oxidation threshold (~ -5.2 eV to -5.3 eV) to achieve long lasting lifetime [42]. Besides, device engineering can also provide the extrinsic stability through sophisticated protection of the conjugated polymer from air and humidity.

2.2.4.5. Appropriate HOMO/LUMO Energy Level

The Highest Occupied Molecular Orbital (HOMO) and Lowest Unoccupied Molecular Orbital (LUMO) of the polymer should be carefully designed for several considerations. Firstly, the HOMO energy level of a material, which determines the accessibility of the material molecule to be oxidized, manifests the air stability of the material. Secondly, the maximum open circuit voltage (V_{oc}) is mainly related to the difference between the LUMO energy level of PCBM and the polymer's HOMO energy level based on experimental evidence [43]. Therefore, in order to achieve high V_{oc} in the device, the polymer donor should have reasonably low lying HOMO level. Figure 8 shows optimal HOMO/LUMO energy level of a typical polymer used in BHJ solar cell with $PC_{60}BM$ as acceptor.

For efficient electron transfer from the polymer donor to the PCBM acceptor in the BHJ blend, the LUMO energy level of the polymer material must be positioned above the LUMO energy level of the acceptor with a minimum separation of 0.2 - 0.3 eV [43]. As shown in Figure 8, the ideal polymer HOMO level should range from -5.2 eV

to -5.8 eV against vacuum level to compromise the air stability, bandgap and open circuit voltage. The ideal polymer LUMO level should range from -3.7 eV to -4.0 eV against vacuum level to facilitate electron injection from polymer to acceptor [44].

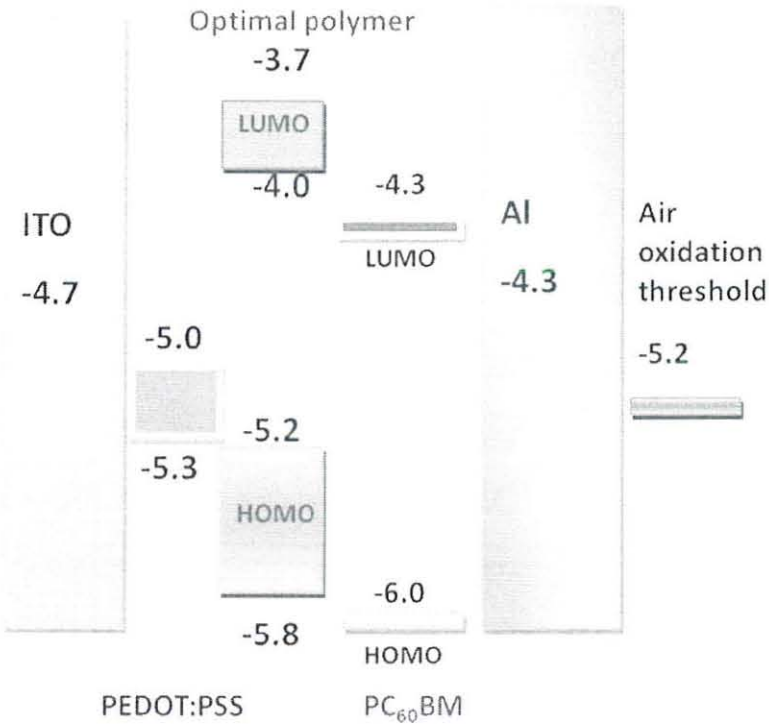

Figure 8. Optimal HOMO/LUMO energy level of an optimal polymer used in BHJ solar cell with $PC_{60}BM$ as acceptor.

2.2.4.6. Optimized Blend Morphology with Fullerene Derivatives

The idea that morphology of the photoactive layer can greatly influence the device performance has been widely accepted and verified by literature reports [45, 46]. However, it is still a 'state-of-art' to control the morphology of specific polymer/PCBM blend. In spite of many reports on different techniques to efficiently

control morphology, the knowledge of device structure-morphology relationship is still in its embryonic stage. Nevertheless, several reliable and efficient methods have been developed in laboratories to improve the morphology as well as the performance of the solar cell devices [47].

One strategy is to control the solvent evaporation process by altering the choice of solvent, concentration of the solution and the spinning rate. The slow evaporation process assists in self-organization of the polymer chains into a more ordered structure, which results in an enhanced conjugation length and a bathochromic shift of the absorption spectrum to longer wavelength region. It is reported [48] that chlorobenzene is superior to toluene or xylene as the solvent to dissolve polymer/PCBM blend during the film casting process. The better solubility of PCBM in chlorobenzene suppresses the tendency of PCBM molecule to form clusters. The undesired clustering of PCBM molecules will decrease the charge carrier mobility of electrons because of the large hopping boundary between segregated grains.

2.2.4.7. High Solubility

A polymer to be used for solar cell application should possess reasonable solubility to be analyzed by solution based characterization methods. Meanwhile, polymers with poor solubility may be inappropriate for solution processing and device performance normally declines due to unfavorable microscopic morphology of the thin film prepared by spin coating. Aliphatic chains attached to the polymer backbone are essential to ensure solubility of the polymer. However, it should be clear that these electronically aliphatic inactive chains will dilute the conjugated part of the polymer and ultimately may reduce the effective mass of the polymer. Some rules of thumb

regarding the use of alkyl chains include that: 1) longer chain is better than shorter chain to solubilize polymer; 2) branched chain is better than linear chain to solubilize polymer; and 3) the more rigid or planar the polymer backbone is, the more or longer alkyl chains are needed [49].

2.3. Characterization of a Solar Cell Devices

The following are often used to characterize solar cells:

a) **Open-Circuit Voltage (Voc)**

V_{oc} is the maximum possible voltage across a photovoltaic cell; the voltage across the cell in sunlight when no current is flowing. If a cell is placed in an open-circuit and illuminated, electrons and holes separate and flow towards the low and high work function materials, respectively. At some point the charge build-up and will reach a maximum equal to the V_{oc}. At the open-circuit voltage, the net current J is zero. For the ideal diode, the V_{oc} increases logarithmically with light intensity. and is given by:

$$\mathbf{V_{oc}} = \frac{\mathbf{nkT}}{\mathbf{q}} \mathbf{ln}\left(\frac{\mathbf{J_{sc}}}{\mathbf{J_0}} + \mathbf{1}\right) \qquad (1)$$

Where n is the diode ideality factor (typically between 1 and 2); J_o is the saturation current density of the diode (caused by diffusion of minority carriers from the neutral region to the depletion region); q is the elementary charge, 1.6×10^{-19} C; k is Boltzman constant of value 1.38×10^{-23} J/K, T is the Kelvin temperature of the cell and J_{sc} is light generated current density.

The equivalent circuit commonly used to interpret the I-V characteristics of solar cells consists of a photogenerator connected in parallel with a diode, which represents the I-V characteristics in the dark. This corresponds to an ideal model in absence of parasitic resistances (R_s and R_{sh}). Figure 9(b) represents the equivalent circuit of a solar cell, where R_s is a series resistance, and R_{sh} is shunt resistance both of which depend on electrode/organic interface properties.

In general, V_{oc} is limited by several factors including interfacial energy levels, shunt losses, interfacial dipoles, and morphology of the active film. For donor/acceptor based solar cells with Ohmic contacts, V_{oc} is mainly determined by the difference between the HOMO of the donor polymer and the LUMO of the acceptor molecule indicating how much the electronic levels are crucial in determining the efficiency of such solar cells.

b) Short-Circuit Current (I_{sc})

I_{sc} is the current that flows through an illuminated solar cell when there is no external resistance (i.e. when the electrodes are simply connected or short-circuited). The short-circuit current is the maximum current that a device is able to produce. Under an external load, the current will always be less than J_{sc}. Factors that lower short circuit current are mainly due to the spectral mismatch between the sunlight and the absorption spectrum of the polymers and fullerenes used, as well as the limited transport of the separated charge carriers to the electrodes due to the low charge carrier mobility in organic materials.

c) Maximum Power Point (mpp)

Thhis is the point (I_{mpp}, V_{mpp}) on the I–V curve where the maximum power is produced. Power (P) is the product of current and voltage (P = IV) and is illustrated in Figure 9 as the area of the rectangle formed between a point on the I–V curve and the axes. The maximum power point is the point on the I–V curve where the area of the resulting rectangle is largest.

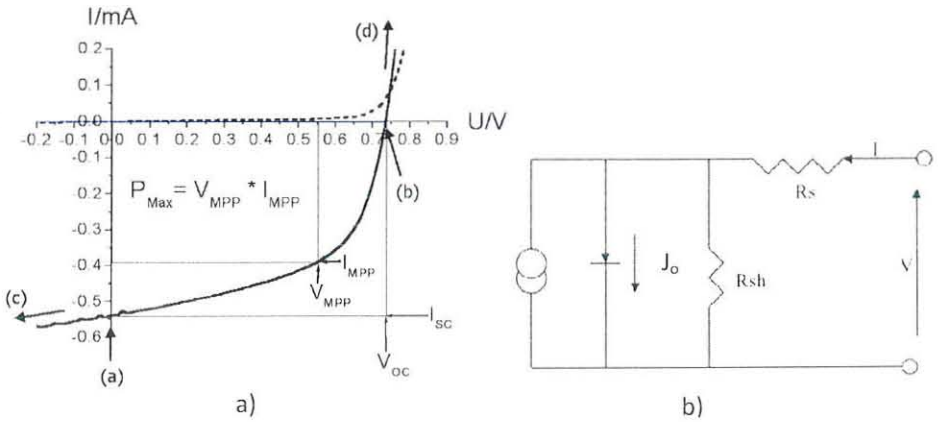

Figure 9. (a) Current–voltage characteristics of a polymer solar cell under illumination (*solid line*) and in the dark (*broken line*), (b) Equivalent circuit of solar cell.

d) Fill Factor (FF)

It is described as the ratio of a photovoltaic cell's actual maximum power output to its theoretical power output if both current and voltage were at their maxima, I_{sc} and V_{oc}, respectively. This is a key quantity used to measure cell performance. It is a measure

of the squareness of the I–V curve. The formula for FF in terms of the above quantities is derived from Figure 9(a).

$$\mathbf{FF} = \frac{\mathbf{I_{mpp}V_{mpp}}}{\mathbf{I_{sc}V_{oc}}} \qquad (2)$$

For a high FF, two things are required: (i) the shunt (parallel) resistance of the diode should be very large to prevent leakage currents, and (ii) the series resistance should be very small to get a sharp rise in the forward current [50].

e) Power Conversion Efficiency (PCE, η)

The ratio of power output to power input. In other words, PCE measures the amount of power produced by a solar cell relative to the power available in the incident solar radiation (P_{in}). P_{in} here is the sum overall wavelength range and is generally fixed at 100 W/cm^2 when solar simulators are used. From Figure 9, the calculation of the power conversion efficiency, η, can be derived. Only the fourth quadrant of the *I–V* curve represents deliverable power from the device. One point on the curve, denoted as maximum power point (MPP), corresponds to the maximum of the product of photocurrent and voltage and therefore power. The ratio between V_{mpp}*I_{mpp} (or the maximum power) and V_{oc}*I_{sc} is called the fill factor (FF), and therefore the power output is written in the form: $P_{max} = V_{oc} \cdot I_{sc} \cdot FF$.

$$\boldsymbol{\eta} = \frac{\mathbf{I_{mpp}V_{mpp}}}{\mathbf{P_{in}}} = \frac{\mathbf{I_{sc}V_{oc}FF}}{\mathbf{P_{in}}} \qquad (3)$$

f) Quantum Efficiency (QE)

QE is the efficiency of a device as a function of the energy or wavelength of the incident radiation. For a particular wavelength, it specifically relates the number of charge carriers collected to the number of photons shining on the device. Quantum efficiency alone is not the same as overall energy conversion efficiency, as it does not convey information about the fraction of power that is converted by the solar cell. QE can be reported in two ways: external QE and internal QE.

External Quantum Efficiency (EQE) – also called incident monochromatic photon-to-current conversion efficiency (IPCE). This type of quantum efficiency includes losses by reflection and transmission. It is defined as the ratio of the number of collected charge carriers to the number of incident photons at a specific wavelength. It is given by the equation:

$$IPCE = \frac{1240 J_{sc}}{\lambda I_{ph}} \qquad (4)$$

Where J_{sc} is short circuit current density ($\mu A/cm^2$), λ the incident photon wavelength (nm) and I_{ph} the incident photon intensity (W/m^2).

Internal Quantum Efficiency (IQE) – is the ratio of the number of charge carriers collected by the solar cell to the number of photons of a given energy that shine on the solar cell from outside *and* are absorbed by the cell. The IQE is always larger than the

EQE. A low IQE indicates that the active layer of the solar cell is unable to make good use of the photons. To measure the IQE, one first measures the EQE of the solar device, then measures its transmission and reflection, and combines these data to infer the IQE.

2.4. Methods to Control the Morphology of BHJ PV Cells

The idea of bulk-heterojunction is used to overcome the short exciton diffusion distance. The photoactive film of heterojunction is formed from the donor and acceptor materials which should be phase-separated on the nanometer length scale, to facilitate the photo-induced charge transfer as well as create interconnected percolating pathways for charge transport to the electrodes. Therefore, the nanomorphology of polymeric solar cells plays a key role for the performance of the devices. Historically, thermal annealing of the film has been used to induce the phase separation between donor and acceptor in bulk-heterojunction blends [51]. However, thermal treatment creates an additional fabrication step in the whole device fabrication process. Later, various methods have been tested and employed to control the nanomorphology of the blends, namely use of solvents with different boiling points (choice of solvent), reduction of drying speed (rate of drying and vapour annealing), changing the solubility of materials, melting of bilayers and the use of processing additives. The later method has got great interest as it removes the need for post-production treatment while at the same time allowing fine control of the nanomorphology in various donor-acceptor blends. The formation and the size of nanoscale domains of donor and acceptor phases are strongly dependent on the film fabrication techniques and conditions. Beyond the selection of suitable materials,

there are several parameters that must be carefully controlled when fabricating BHJ solar cells, such as the solution concentration, deposition temperature, donor-acceptor blend ratio, spin speeds using solvents with different boiling points and solubility. Methods, such as reducing the drying speed of spin-coated films and solubility matching have also been used. It has been observed that chemical additives can substitute the post production treatment of BHJ solar cells [52]. Use of processing additives is an attractive concept due to the simplicity and suitability for large scale production.

2.4.1. Thermal Annealing of Devices

Thermal annealing is based on controlling the temperature and annealing time; and is employed to either the final device or BHJ films in order to improve the nanoscale phase separation between donor and acceptor. Significant improvement in photovoltaic performance after annealing is typically observed in P3HT/PCBM blends [24]. Thermal annealing has the advantage in that it can be applied independently of the film deposition technique. Thermal annealing has also been shown to enhance the crystallinity of the polymer, such as for P3HT, increasing the PCE and the photocurrent due to increased carrier mobility [39]. Furthermore, the interconnections between the polymer/fullerene phases in the interpenetrating network are enhanced as a result of phase separation between the donor and acceptor on meso (> 100 nm) and nanoscales (< 20 nm).

2.4.2. Solvent Effects

Postproduction treatment requires a rather well controlled environment, it adds an additional fabrication costs to the solar cell manufacturing process, which might not be attractive for large-scale industrial production. Phase separation and molecular self-organization can be influenced by solvent evaporation since the solvent establishes the film evolution environment. Slow drying or solvent annealing (creating an atmosphere of the solvent by confining the system) techniques have also been used to control the morphology of the blends by changing the rate of solvent removal. Higher PCE values due to improved film morphology and crystallinity have been reached by substituting chloroform with chlorobenzene for P3HT/PCBM BHJ solar cells. The difference between chlorobenzene and 1,2-dichloro benzene for use as a solvent was shown and chlorobenzene resulted in films with higher roughness [31].

2.4.3. Processing Additives

This method is based on the usage of non-reacting chemical additive or processing solvent additive, to the donor and acceptor solution. It was demonstrated that the addition of DHPT3 in P3HT/PCBM thin films induces a structural ordering of the polythiophene phase, leading to improved charge carrier transport properties and stronger active layer absorption [39]. The incorporation of other solvents into the host solvent is capable of controlling the film morphology. In some cases, changes in the solvent composition lead to interchain order that cannot be obtained by any other method. The use of nitrobenzene as an additive has been shown to improve the phase-separation between the donor and acceptor (P3HT/PCBM blend), where P3HT was shown to be present in both amorphous and crystalline phase [41].

Though several different bulk-heterojunction approaches are investigated, those employing a conjugated polymer such as, OPV processing additives, offer an attraction over annealing processes in that they do not require an additional fabrication step. Two general guidelines for additive design are as follows: (1) the boiling point must be significantly greater than that of the processing solvent to maximize the interaction time between the additive and the active layer components during thin film formation, and (2) one active layer component must be significantly more soluble in the additive than the other component. Recent promising additives fulfilling these guidelines include di(X)octanes, where X is a small, polarisable group such as a halogen. For BHJ systems containing donor polymers di-iodooctane (DIO) affords the largest PCE enhancements observed to date. Several studies reveal that processing additives promote more favourable BHJ morphologies [22], little is understood about the microstructural evolution occurring in the transformation from solution-phase BHJ precursors to thin photoactive films. Figure 10 shows the effect of processing additive on BHJ morphology.

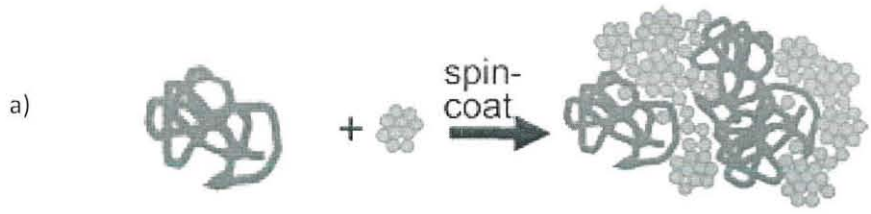

Processed without additive

b)

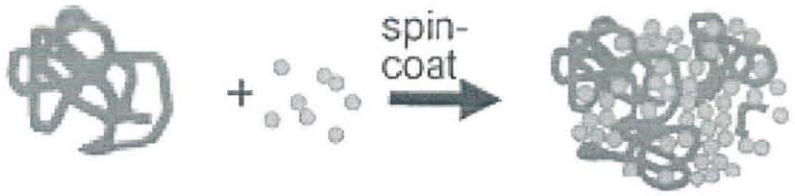

Processed with additive

Figure 10. Schematic diagram showing the effect of processing additive (a-b).

3. Objectives

3.1. General objectives

- To study the effect of solvent additives (like iodobutane, diiodomethane, iodomethane and iodoethane) on the photovoltaic parameters of PDTSTTz:PCBM based BHJ solar cells, and the effect in the performance after the introduction of P3HT into PDTSTTz/PCBM system as a third component.

3.2. The specific objectives

- To construct organic BHJ solar cells based on PDTSTTz:PCBM containing each of the solvent additives (iodobutane, diiodomethane, iodomethane and iodoethane),
- To characterize the solar cells using various standard characterization techniques such as I-V, IPCE, UV-Vis.

- To compare the relative effect of each additives on the photovoltaic parameters of the BHJ solar cells.
- To compare the PCE of devices spin-coated with/and without solvent additives,
- To qualitatively and quantitatively explain the changes in the photovoltaic properties caused by solvent additives,
- To characterize the effect of introducing P3HT on the performance of PDTSTTz/PCBM BHJ solar cells.

4. Experimental

4.1. Materials

i. Donor semiconducting conjugated polymers

The following conjugated electron donor polymers were obtained from collaborators and used as light absorbing active layer in the bulk heterojunction solar cell devices.

a)

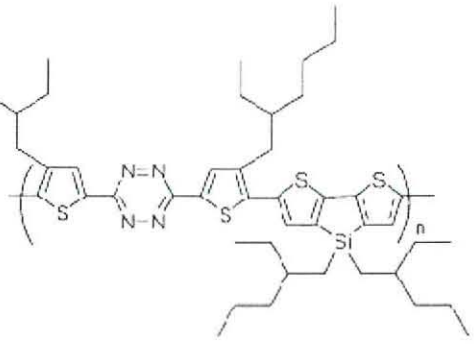

PDTSTTz

b)

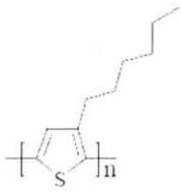

RR-P3HT

Figure 11. Molecular structure of: a) poly[2,6-(4,4'-bis(2-ethylhexyl)dithieno[3,2-b:2',3'-d]silole)-alt-5,5'-(3,6-bis[4-(2-ethylhexyl)thienyl-2-yl]-s-tetrazine)], PDTSTTz, b) poly(3-hexylthiophene), P3HT (Reike).

ii. PEDOT:PSS and PCBM

Poly(3,4-ethylenedioxythiophene)/poly(styrenesulfonate) (PEDOT/PSS) (Baytron PH) is used as a hole conducting material in the bulk hetrojunction solar cells studied. [6,6]-phenyl-C61-butyric acid methyl ester (PCBM) (from SOLENE) was used as an acceptor in the bulk heterojunction solar cell devices studied.

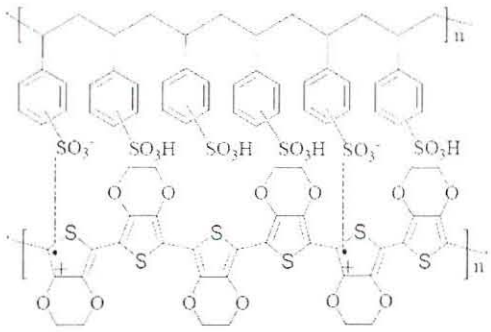

a) PEDOT:PSS

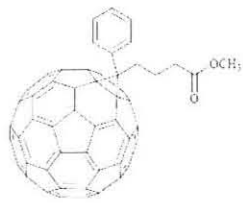

b) PCBM

Figure 12. *Chemical structures of a) PEDOT:PSS b) PCBM.*

iii. Other inorganic materials and solvents

Aluminium metal and Indium doped tin oxide (ITO) coated glass as cathode and anode, respectively; and standard solvents such as ethanol, acetone, isoprpanol, and di-chlorobenzene were used.

iv. Solvent Additives

Solvent additives used in this work include di-iodomethane (DIMe), iodomethane (IMe), iodoethane (IEt) and iodobutane (IBu).

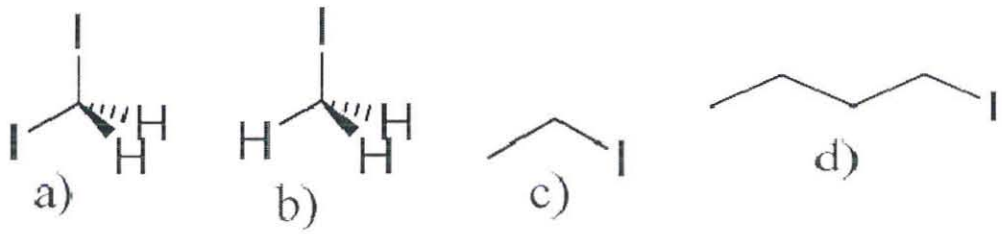

Figure 13. Molecular structure of; a) di-iodomethane, b) iodomethane, c) iodoethane, d) iodobutane.

Table 1. Physical properties of the host solvent and solvent additives used [11].

Solvent	Mol. Weight (g/mol)	Boiling point, (°C)	Dielectric constant
Di-chlorobenzene	146	178	9.9
Di-iodomethane	268	181	8.9
Iodomethane	142	42	7.0
Iodoethane	156	72	7.4
Iodobutane	184	119	4.5

4.2. Sample Preparation

For absorption experiments, thin films prepared by spin coating on a transparent glass slides were used. PDTSTTz and PCBM in an optimal 1:1 ratio [16] were dissolved in di-chlorobenzene with a concentration of 10 mg/mL. The same concentration was used in all absorption measurements of devices.

For I-V characteristic measurements, bulk heterojunction type solar cells were constructed from solutions which were prepared with appropriate mixture ratios of polymer or polymer/polymer mixtures to the acceptor PCBM in di-chlorobenzene with a concentration of 10 mg/mL (for all measurements) stirred overnight. The indium tin oxide (ITO) coated glass substrates were first cleaned by ultra-sonication in Ultrasonic bath (Decon, FS100b) successively with glass acetone and isopropanol, and dried in air. Filtered PEDOT/PSS (Baytron PH) was spin coated using spin-coater

(P6700) on top of ITO with 2000 - 4000 rpm and was baked at 140°C on a hotplate for 15 minutes. The active layer (polymer:PCBM) solution containing 2.5% (v/v) each of the different additives mentioned earlier, was then spin-coated on top of PEDOT:PSS film at 800 RPM. Then the samples were dried in air. The top electrode aluminum metal (~97 nm) deposition was done using thermal evaporator (EDWARDs 306) in vacuum of about 5×10^{-6} mbar. A devices with a configuration of *ITO/PEDOT:PSS/PDTSTTz:PCBM/AL(97 nm)*, with active area ~ 4 mm^2 were obtained.

4.3. Mesurements and Instruments

The thin film absorption spectra were recorded using UV-Vis Spectrophotometer (Spectronic Genesis, 2PC, USA) from 300 – 800 nm wavelength range. For the photoelectrochemical solar cells I-V characteristics, an electrochemical analyzer under illumination of white light 100 mW/cm^2 (adjusted by Gigahertz-Optik -X11 Optometer) from a 150 W halogen lamp by an Oriel light source (Model 68830) was used. For IPCE, a grating monochromator (Model 77250) placed into the light path was used to select a wavelength between 300 and 800 nm. The photocurrent spectra responses of the lamp were corrected using a standard silicon photodiode (Hamamatsu, Model S1336-8BK).

5. Results and Discussion

5.1. UV- Visible Absorption of PDTSTTz:PCBM

Based on the strong dependency of solid-state UV-Vis absorption of conjugated polymers on their molecular packing, we investigated the absorption spectra of PDTSTTz:PCBM (1:1) films processed from short chain iodoalkane/ di-iodoalkane solvent additives and their effect on the photovoltaic parameters of the devices. Here, one of the criteria for processing additives introduced to control the morphology of bulk heterojunction (BHJ) materials for use in solar cells has been identified: selective (differential) solubility of the fullerene component. A possible explanation is that the iodine atom bears a partial negative charge and PCBM is electro-deficient, which may be the reason for their relatively strong interactions with each other and the enhanced solubility of PCBM in the presence of additive [20]. Using this criterion, we have investigated the class of iodoalkanes (IMe, IEt, IBu) and di-iodoalkane (DIMe) as processing additives for PDTSTTz/PCBM based BHJ solar cells.

To mimic BHJ solar cell fabrication conditions, the concentrations of the active layer components used were the same as those for optimized devices. Depicted in Figure 14, is the UV-Visible absorption spectra of PDTSTTz:PCBM films processed in di-chlorobenzene containing 2.5% (v/v) of each of di-iodomethane (DIMe), iodobutane (IBu), iodoethane (IEt), and iodomethane (IMe) solvent additives and pristine PDTSTTz:PCBM (without additive). The absorption spectra (shown in Figure 14) indicated that in the presence of these solvent additives, devices generally exhibited a slight shift in their absorption maximum to the longer wavelength relative to the pristine devices. This might be for the reason that, in the presence of solvent additives, PCBM aggregates will dissolve and well segregate throughout the polymer chain. This will cause the polymer chains to redistribute thereby improving their crystalline order [26]. The segregation of the relatively well dissolved PCBM molecules causes twisted polymer chains to be stretched. Besides, with penetration of the PCBM molecules, polymer chains will get the chance to align together and form a crystalline order within the film. All these increase the effective conjugation length that reduces the bandgap with an ultimate effect of red-shift in the absorption spectra.

Solubility effect of additive to PCBM increases with increasing alkyl chain length. One rule of thumb is that long chain is better than short chain to solubilize polymer [49]. This can also be assigned to a significant red-shift (by ~ 14 nm) in the films which were processed from iodobutane additive. Besides, strong chain interactions improve the crystallinity that will increase the facilitation in the formation of crystalline PDTSTTz domain with improved phase separated morphology in the blend film [18].

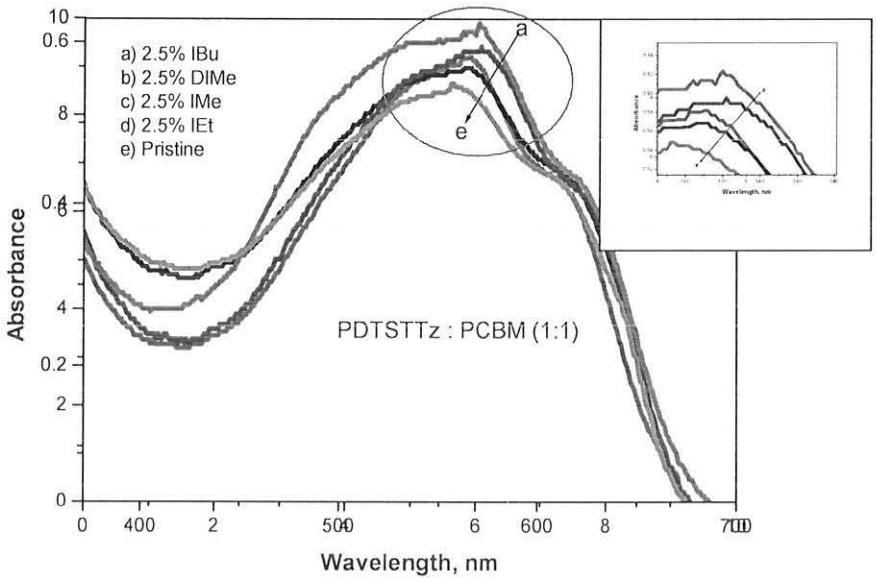

Figure 14. Absorption spectra of PDTSTTz:PCBM thin films spin coated on transparent glass slides at 800 RPM processed from 10 mg/mL of pure DCB, and DCB containing 2.5% (v/v) of each of the solvent additives; a) IBu, b) DIMe, c) IMe, d) IEt, and e) Pristine.

5.2. Current Density-Voltage (J-V) Characteristics of PDTSTTz:PCBM

To directly evaluate the effect of additives on the overall device performance, the J–V characteristics of all the solar cell devices constructed were measured under 100 mW/cm^2 white light illumination in air. The J–V plots for all devices are depicted in Figure 15. The calculated values of the solar cell parameters are summarized in Table 2. As clearly evident in Figure 15, the device fabricated with iodobutane solvent additive exhibited high J_{sc} (6.13 mA/cm^2) and improved performance (PCE = 2.02%) and a fill factor (FF) that increased up to 0.47; compared to the pristine device with a PCE of 0.39%. The improvement is primarily due to the increase in the short circuit current and fill factor which was believed to arise from distinct and separated morphology [18]; and a slightly improved PDTSTTz crystallinity. The red-shifted absorption enabled to collect more low energy photons; and the improved morphology facilitated carrier mobility [18]. These factors, in turn, might have led to enhanced J_{sc} in the blend films. In contrast, the devices prepared with iodomethane and iodoethane additives yielded relatively lower J_{sc} values which led to lower PCE% (0.51 and 0.93, respectively). This is due to the low photocurrent, which is in turn might be attributed to limitations in the charge transport and collection. The molecular packing of the conjugated polymer turned out to largely influence on serial (bulk) resistance, R_s, of the OPV [21]. This allows more efficient charge transport to increase the FF from 0.33 to 0.47 in the presence of IBu. Besides, more interestingly, in di-iodomethane processed device with J_{sc} of 4.90 mA/cm^2, a FF of 0.48 was observed, which led to a second highest overall PCE of 1.6%. This highly improved PCE in di-iodomethane compared to the corresponding iodomethane might be because of the presence of extra polarisable iodine atom in di-iodomethane that creates strong

interaction to solublize PCBM aggregates and its high boiling point (slow drying effect) than IMe that ultimately led to enhanced crystallinity of of PDTSTTz chains.

Here we obtained a PCE of 2.02% for PDTSTTz/PCBM system which is lower than the reported value of 5.59% [13]. This is basically because we did all the preparations and measurements in an open environment (in contact with air) that lowered the efficiency. Nevertheless, our results could adequately explain the effect of solvent additives on the PV parameters.

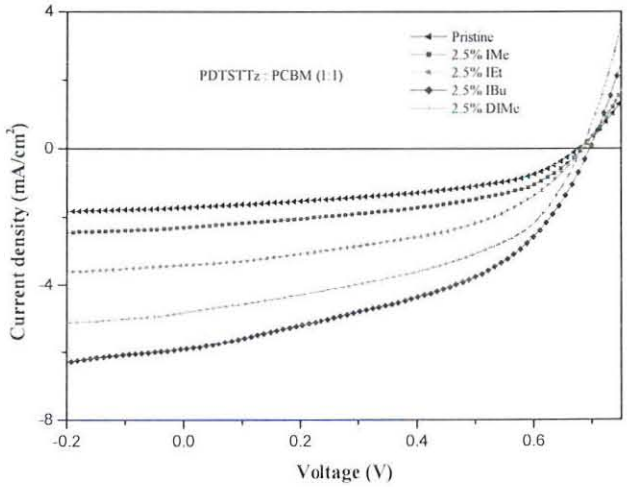

Figure 15. J-V curve of ITO/PEDOT:PSS/PDTSTTz:PCBM/Al(~97 nm) solar cells processed in pure DCB, and DCB containing 2.5% (v/v) of solvent additives under 100 mW/cm^2 white light illumination. The concentration of solution was 10 gm/mL, spin coated at 800 RPM.

In general, without additive, the PCBM aggregates might be large which hinders PCBM intercalation into the PDTSTTz network during film formation, so that large, segregated domains form. However, on addition of additive, the PCBM aggregates

dissolve following the selective solubility effect of solvent additives to PCBM. This facilitates integration of the PCBM molecules into the PDTSTTz aggregates. Therefore, the increased efficiencies must result from an increase in the mobile-carrier-generation efficiency and an increase in the mobile-carrier lifetime as a result of changes in the heterojunction morphology. The strong dependence of the absorption, the morphology and the device performance on the alkyl chain length implies that long chain processing additives influence the physical interactions between the polymer chains and/or between the polymer and fullerene acceptor [18].

However, the V_{oc} did not essentially change which might be due to the balanced effect of enhanced ordered crystalline that causes a slight decrease in V_{oc}, and of the improved phase separated morphology that has a positive effect on V_{oc}. As ordered crystalline PDTSTTz domain is formed the effective conjugation length increased and the HOMO-LUMO gap decreased leading to a slight decrease in V_{oc}. On the other hand, well phase-separated morphology is favourable for charge dissociation and transport that may lead to a slight increase in V_{oc}. When these counteracting effects get balanced, the V_{oc} may not show a significant change. Then, it can be said that iodoalkane solvent additives provide an improvement in J_{sc}, FF, and hence the overall solar cell performance (with no essential change in V_{oc}), in two ways: efficient light harvesting by improved PDTSTTz crystalline order and enhanced charge transport and offering a better morphology. A five-fold PCE increase was observed for IBu (see Table 2).

Table 2. Summary of the solar cell device performance for the ITO/PEDOT:PSS/PDTSTTz:PCBM/Al(97 nm) active layer containing different additives.

Sample	J_{sc} (mA/cm^2)	V_{oc} (V)	FF	PCE%
Pristine	1.76	0.67	0.33	0.39
2.5% IMe	2.35	0.68	0.32	0.51
2.5% IEt	3.63	0.68	0.38	0.94
2.5% IBu	6.13	0.70	0.47	2.02
2.5% DIMe	4.90	0.68	0.48	1.60

The effect on photovoltaic properties of BHJ devices based on PDTSTTz:PCBM blends was also observed in the external quantum efficiencies (EQEs) measurement which is given in Figure 16. Devices, which were processed from solvent additives also showed IPCE improvement in the longer wavelength region, when compared to the pristine device (with no additives) with significant effect in di-iodomethane and iodobutane as shown in Figure 16. Some devices exhibited a relatively low IPCE value eventhough they have good absorption at longer wavelengths, which may be due to the limited charge transport that may be related to the occurrence of unoptimized phase separation. The profound improvement in the IPCE, with the addition of different additives is believed to increase both the optical absorption and the charge transport, as well as reduce recombination losses due to improvements in crystallinity and film morphology [18]. Therefore, the attained IPCE results are in good agreement with the trends observed in the optical absorption spectra and the calculated device parameters.

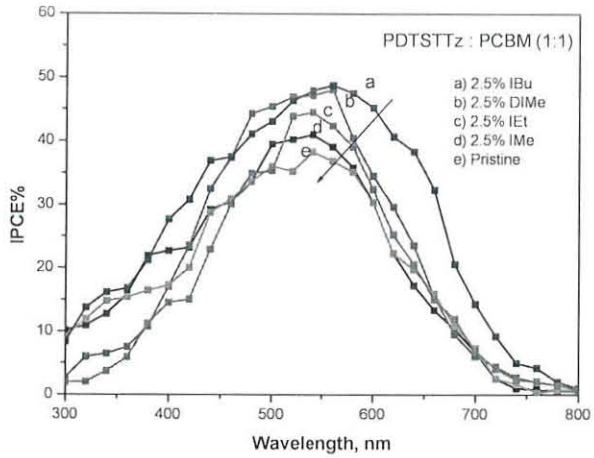

Figure 16. Incident photon-to-current conversion efficiency (IPCE) spectra of the ITO/PEDOT:PSS/PDTSTTz:PCBM/AL(~97 nm) devices processed in pure DCB, and DCB containing 2.5% (v/v) of solvent additives: a) IBu, b) DIMe, c) IEt, d) IMe, and e) Pristine. All devices spin coated at 800 RPM from 10 mg/mL solution.

5.3. Effect of P3HT on Photovoltaic Parameters of PDTSTTz/PCBM Devices

Here the effect on the photovoltaic parameters was investigated after the introduction of a second donor, P3HT, into a PDTSTTz/PCBM system. We used the UV-Vis spectra (see in Figure 15) of the respective P3HT/PCBM and PDTSTTz/PCBM binary blends as a clue to extend our investigation. PDTSTTz has a broad absorption band predominantly between 500 and 650 nm, whereas P3HT absorbs at relatively shorter wavelengths, between 400 and 550 nm. The addition of P3HT into PDTSTTz/PCBM system was based on the expectation of two possible advantages:

a) To cover the absorption hollow (as P3HT and PDTSTTz maximally absorb in different region), thus both thermalization and transmission loses can greatly be minimized.

b) The compatibility with the HOMO/LUMO levels of PDTSTTz and of hole transporting layer, PEDOT, may improve hole extraction.

The UV-Vis spectra indicated in Figure 17 has clearly shown that the addition of P3HT resulted in the broadening of absorption region. This is due to the combining effect of the two polymers that contribute to increase the absorption coverage (area).

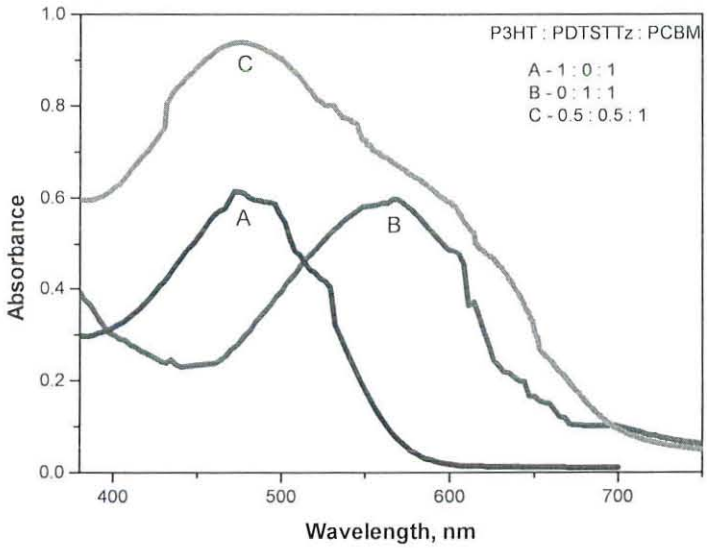

Figure 17. UV-Vis absorption spectra of P3HT/PCBM, PDTSTTz/PCBM and P3HT/PDTSTTz/PCBM films spin coated on a transparent glass slides from 10 mg/mL solution in pure DCB at 800 RPM.

The energy level of each of the components is depicted in Figure 18.

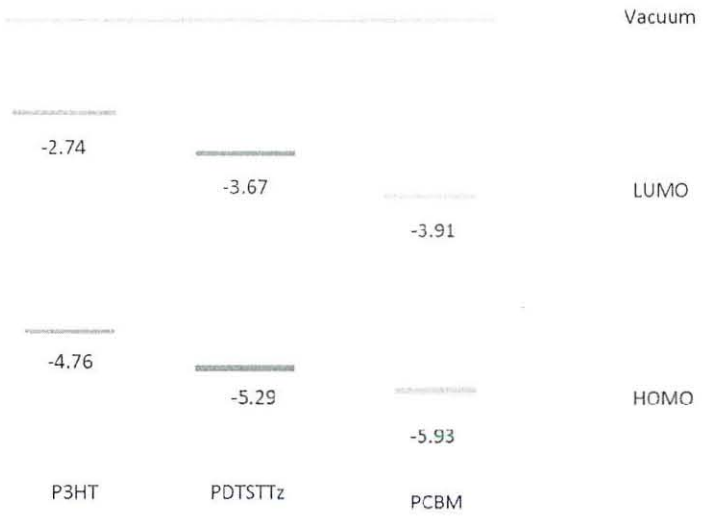

Figure 18. Relative HOMO/LUMO levels of P3HT, PDTSTTz and PCBM.

Then the best performing P3HT/PDTSTTz composition was optimized for the same PCBM level in the P3HT/PDTSTTz/PCBM blend as explained next.

5.3.1. Optimization of P3HT/PDTSTTz

Photovoltaic devices containing P3HT/PDTSTTz/PCBM (ternary) blends in the conventional device configuration ITO/PEDOT:PSS/P3HT:PDTSTTz:PCBM/Al(97 nm) were fabricated in air. In order to compare the device parameters, the concentration of all polymer/fullerene solutions was kept constant (10 mg/mL), and spin coated at 800 RPM. Furthermore, in all cases the overall polymer:fullerene weight ratio was maintained at 1:1. Accordingly, compositions of 25%, 50% and 75% (w/w) of P3HT with respect to PDTSTTz were introduced to form a blend of P3HT/PDTSTTz/PCBM solution in di-chlorobenzene in the presence of 2.5% IBu as

a phase separating agent. Then devices were constructed and characterized for their J-V response as depicted in Figure 19(a). Table 3 lists the values of J_{sc}, V_{oc}, FF, and PCE% obtained under illumination of 100 mW/cm^2 as the P3HT:PDTSTTz ratio was varied.

Also for comparison, binary OPVs with P3HT/PCBM or PDTSTTz/PCBM composite ratio of 1:1 (w/w) were constructed and characterized under the same conditions. Then, it was observed that the PDTSTTz:PCBM binary blend displayed, Jsc = 6.13 mA/cm^2, V_{oc} = 0.7 V and FF = 0.47, giving an efficiency of 2.02%, and the P3HT:PCBM binary blend showed J_{sc} = 7.01 mA/cm^2, V_{oc} = 0.5 V, and FF = 0.45, giving an efficiency of 1.6%. Combining P3HT, PDTSTTz, and PCBM (forming a ternary blend) could lead to higher J_{sc} for all the ternary blends than for either limiting binary blend as a result of more wider spectral coverage of absorption (as has been demonstrated in Figure 17). The corresponding J-V plot for the relative comparison of binary and ternary systems is given in Figure 20. A significant increase in J_{sc} to 11.08 mA/cm^2 could couple with an intermediate V_{oc} of 0.56 V to give an efficiency of 2.42% at FF = 0.39. The ternary blend could thus give a higher efficiency than either limiting binary blend as a result of the higher attainable $J_{sc}V_{oc}$ product. Combination of P3HT and PDTSTTz in 1:1 ratio might have led to the formation of improved local structure (crystalline order) responsible for better photon harvesting, and by extension higher J_{sc}, than any of the possible compositions. Analogously, a similar observation has been achieved also for the pristine (without additive) results listed in Table 3.

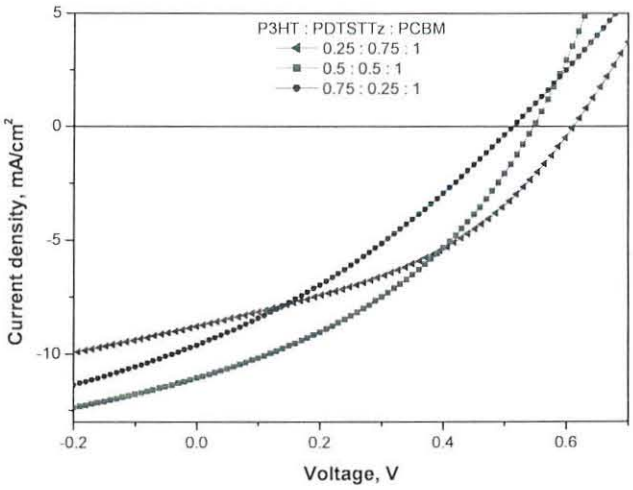

Figure 19. J-V plots for ITO/PEDOT:PSS/P3HT/PDTSTTz/PCBM/Al(97 nm) films with different P3HT/PDTSTTz composition processed from 10 mg/mL solution of DCB containing 2.5% IBu, and spin coated at 800 RPM.

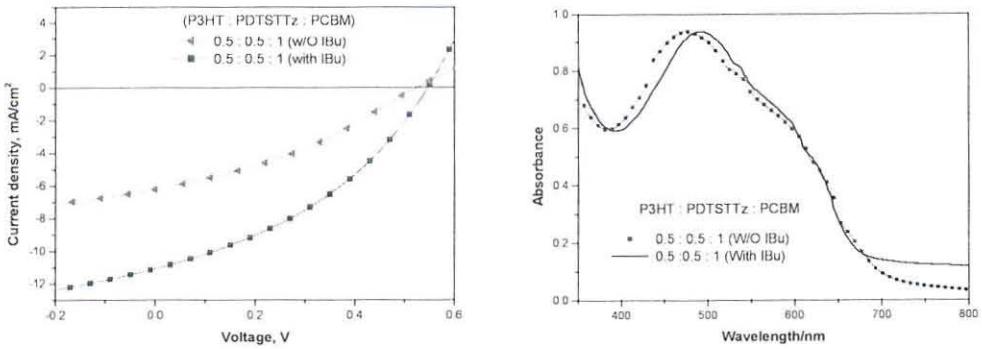

Figure 20. a) J-V plots for ITO/PEDOT:PSS/P3HT/PDTSTTz/PCBM (0.5:0.5:1)/Al(~97 nm) devices, and b) UV-Vis spectra of the P3HT/PDTSTTz/PCBM (0.5:0.5:1) films spin coated on glass slides In both cases, solution concentration is 10 mg/mL in DCB with and without IBu spin coated at 800 RPM.

Thus, as described earlier, the best performing cell consisted of P3HT/PDTSTTz/PCBM (0.5:0.5:1) produced the best efficiency of 2.42%, surpassing that of the corresponding binary cells based on P3HT/PCBM (PCE = 1.6%) or PDTSTTz/PCBM (PCE = 2.02%). The increase in PCE is by 19.8% with respect to PDTSTTz/PCBM and by 51.3% with respect to P3HT/PCBM devices. This observed enhancement originated primarily from improvements in J_{sc}. The increased J_{sc} was attributed to the broad photon absorption contributed by the two donors. The relatively lower FF (0.39) of the ternary device, however, might be due to a relatively unoptimized phase separation following the introduction of a third component in the blend that ultimately causes power loss [34]. However, strong processing additives still have the potential to improve the morphology of ternary systems (as can be noted from Figure 19b, Figure 20 and Table 3).

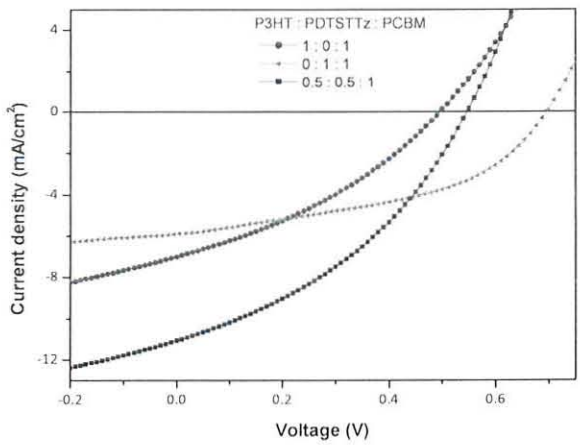

Figure 21. J-V plots of ITO/PEDOT:PSS/P3HT:PDTSTTz:PCBM/Al(~97 nm) (0.5:0.5:1) devices with the corresponding binary ones; all processed from 10 mg/mL DCB solution containing 2.5% IBu; spin coated at 800 RPM.

The IPCE spectra of the ternary cell based on P3HT/PDTSTTz/PCBM for 0.5:0.5:1 optimized ratio showed the contribution of both polymers to the increase in photon-to-current conversion efficiency (see Figure 21) which is consistent with the absorption spectra (in Figure 17).

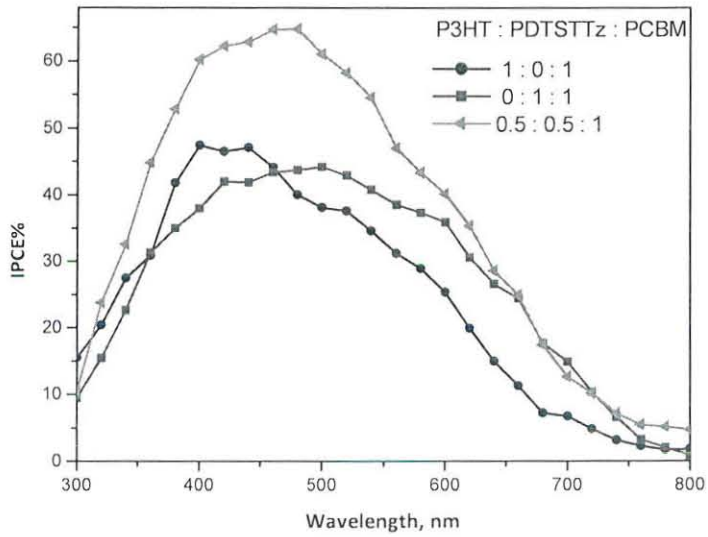

Figure 22. Incident photon-to-current conversion efficiency (IPCE) of the ITO/PEDOT:PSS/P3HT:PDTSTTz:PCBM (0.5:0.5:1)/Al(~97 nm) and the corresponding binary devices processed in DCB containing 2.5% (v/v) of IBu as a phase separating agent. Solution concentration was 10 gm/mL, and spin coating speed 800 RPM.

Table 3. Summary of the solar cell device performance for ITO/PEDOT:PSS/P3HT:PDTSTTz:PCBM/Al(~97 nm) films containing different composition of P3HT and PDTSTTz processed from 10 mg/mL in DCB with 2.5% IBu as a phase separating additive under 100 mW/cm^2 white light illumination.

P3HT :PDTSTTz: PCBM	J_{sc} (mA/cm^2)	V_{oc} (V)	FF%	PCE%
1 : 0 : 1	7.01, 3.43*	0.50, 0.50*	0.45, 0.32*	1.60, 0.57*
0.75 : 0.25 : 1	9.21	0.51	0.37	1.74
0.5 : 0.5 : 1	11.08, 6.22*	0.56, 0.55*	0.39, 0.33*	2.42, 1.13*
0.25 : 0.75 : 1	8.94	0.62	0.39	2.16
0 : 1 : 1	6.13, 1.76*	0.70, 0.67*	0.47, 0.33*	2.02, 0.39*

* Pristine (without processing additive)

Figure 22(a - c) depicts the J_{sc}, V_{oc} and PCE% variations with composition of P3HT or PDTSTTz in P3HT/PDTSTTz/PCBM for the same amount of PCBM in the blend. Several significant observations can also be made from the data in Table 3. Importantly, as is also illustrated in Figure 22(b), V_{oc} of the three-component solar cells showed a gradual decrease from 0.70 to 0.50 V as the amount of P3HT in the ternary blend increased. This establishes that in ternary blend BHJ solar cells, V_{oc} is not necessarily pinned to the V_{oc} of the corresponding binary blends.

The slight decrease in V_{oc} can be assigned to the effect of band bending due to disorder in the three-component system. Vacuum level alignment with flat bands away from the interface is found when the interface hole barrier is larger ($\geq$ 0.6 eV)

[48]. Thus, band bending away from the Fermi level occurs when the hole barrier is smaller than this value. Following the addition of P3HT, which is in ohmic contact with the Fermi level of the ITO with barrier (energy level difference) ~ 0.06 eV (see Figures 8 and 18 for approxomation), interface charges will be injected and excess charge accumulate on the polymer. The resulting field shifts the polymer levels to limit charge penetration in the bulk of the film thereby to reduce the V_{oc} [48]. The V_{oc} attained minimum value (0.5 V) for pure P3HT/PCBM (greater band bending) and maximum value (0.7) for pure PDTSTTz/PCBM with barrier ~ 0.6 eV (little band bending). Besides, the FF almost remains constant for P3HT/PDTSTTz/PCBM based devices (in the presence of P3HT) which might be an evidence for the existence of balanced charge carrier transport. This supports our prediction that with this balanced free charge transport; band bending might be one factor for V_{oc} variation.

Another way of explaining the V_{oc} variation can be in terms of the relative positions of HOMO levels of P3HT and PDTSTTz. PDTSTTz has low lying HOMO level where as P3HT has shallow HOMO level. Hence, maximum V_{oc} is determined by the HOMO of PDTSTTz and minimum V_{oc} by the HOMO of P3HT. Thus, with increasing the amount of P3HT in P3HT:PDTSTTz, the V_{oc} decreases up to the minimum value that corresponds to the pure P3HT.

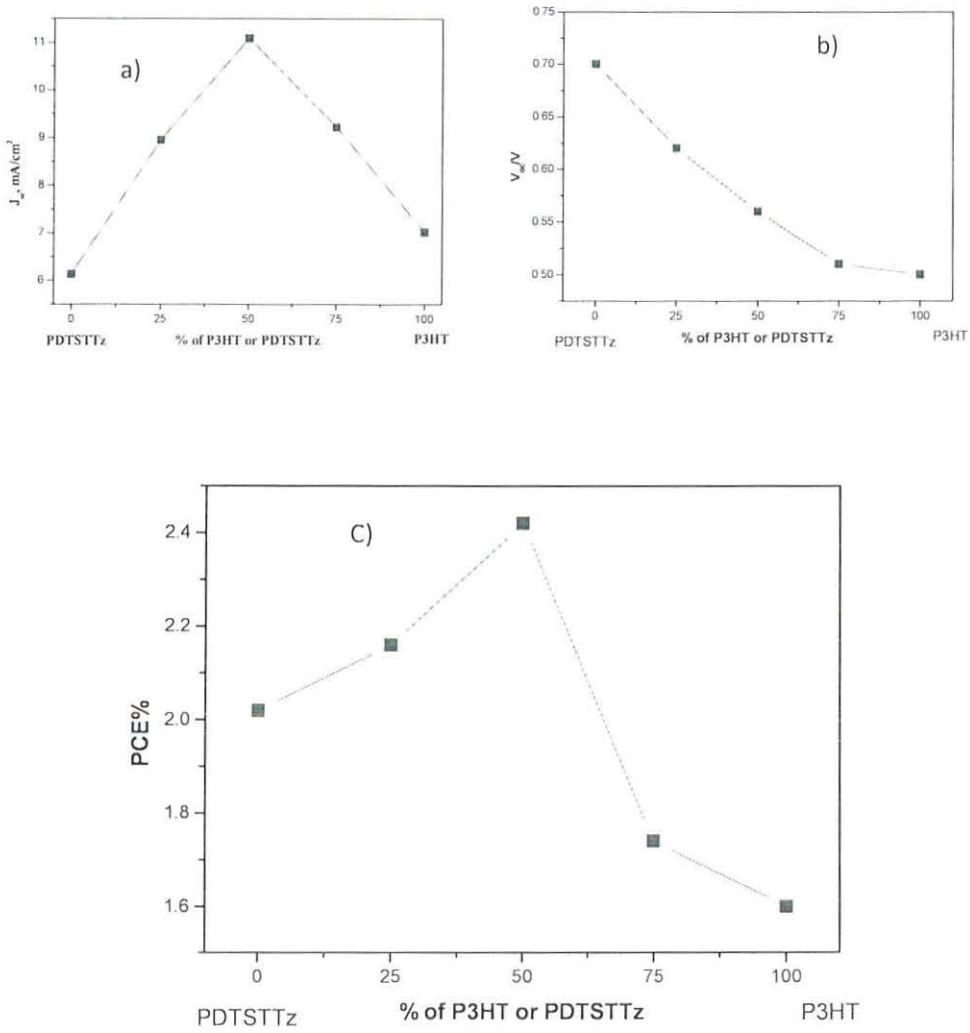

Figure 23. a) J_{sc}, b) V_{oc}, and c) PCE%; as a function of the amount of P3HT for the ternary blend BHJ solar cells

Finally, it is important to note (see Table 3 and Figure 22 (a-b)) that the J_{sc} seems to govern the $J_{sc}V_{oc}$ product and hence the PCE regardless of the V_{oc} change. Thus, J_{sc} improvement is critical for essential improvement in PCE of solar cell devices.

6. Conclusions

We have demonstrated the utility of different classes of processing additives introduced to see the effect on the morphology of PDTSTTz/PCBM BHJ materials for use in solar cells. The control of the BHJ morphology by selective solubility of the fullerene component in the BHJ blend was demonstrated. Using these criteria, the effect of iodomethane, iodoethane, iodobutane and di-iodomethane solvent additives was investigated solely on PDTSTTz/PCBM devices. The UV-Vis absorption spectra of these blend films processed in di-chlorobenzene containing the additives showed a relative red-shift at the characteristic PDTSTTz absorption band when compared to the pristine PDTSTTz/PCBM blend, with better effects observed in iodobutane and di-iodomethane.

From the calculated values of basic parameters, PDTSTTz/PCBM based devices containing iodobutane and di-iodomethane additives exhibited enhanced J_{sc}, FF and PCE. Iodobutane and di-iodomethane yielded J_{sc} values (6.13 mA/cm^2 and 4.90 mA/cm^2, respectively). Iodobutane processed devices gave the highest overeall PCE of 2.02% compared to the pristine device (PCE = 0.39%). As the chain length of alkyl iodide additive increased from iodomethane to iodobutane (C_1 – C_4), the relative device J_{sc}, FF, and PCE increased for PDTSTTz/PCBM devices. Further observation is that the performance of di-iodomethane (PCE = 1.6%) was better than iodomethane (PCE = 0.51%) and was an indication for the enhancing property of di-iodoalkanes, too. This can be attributed to the extra polarisable iodine atom in DIMe that facilitates the fullerene solubility its relatively high boiling point of DIMe favourable for slow film growth.

Thus, further improvement of PDTSTTz/PCBM based device performance is possible by using long chain iodoalkane or di-iodoalkane solvent additives as a phase separating agent for well separated, optimized morphology.

Finally, the addition of a second electron donor (P3HT) into PDTSTTz/PCBM forming a ternary blend with two donor system was investigated. Our results showed high improvement in J_{sc} (11.08 mA/cm^2) and maximized PCE (2.42%) with respect to the single donor systems (P3HT/PCBM or PDTSTTz/PCBM) resulting primarily from the increased (wide range) photon harvesting. This shows that BHJ solar cells with multi-donor system are potential and promising candidates for future polymer based PV applications if morphology is well controlled.

7. References

1. Global Climate and Energy Project, "*An Assessment of Solar Energy Conversion, Technical Assessment Report,*" Stanford University, **2007**, p. 4.
2. C. Deibel, V. Dyakonov; *Rep. Prog. Phys. 73* (**2010**) 1.
3. Z. Bao, W. K. Chan, L. Yu; *J. Am. Chem. Soc. 117* (**1995**) 12426.
4. F. Padinger, R. S. Rittberger, N. S. Sariciftci; *Adv. Funct. Mater. 13* (**2003**) 85.
5. M. A. Green, K. Emery, D. L. King, S. Igari, W. Warta; *Prog. Photovolt. Re. Appl. 13* (**2005**) 387.
6. J. R. Tumbleston, D. - H. Ko, E. T. Samulski, R. Lopez; *J. Appl. Phys. 108* (**2010**) 084514.
7. K. Yu. J. Chen; *Nanoscale Res. Lett. 4* (**2009**) 1.
8. J. L. Bredas, G. B. Street; *Acc. Chem. Res. 18* (**1985**) 309.
9. J. J. M. Halls, K. Pichler, R. H. Friend, S. C. Moratti, A. B. Holmes, *Appl. Phys. Lett. 68 (***1996**) 3120.
10. M. S. Su, C. Y. Kuo , M. C. Yuan , U. S. Jeng , C. J. Su , K. H. Wei; *Adv. Mater. 23* (**2011**) 3315.
11. S. - H. Chan, Y.- S. Hsiao, L.- I. Hung, G. - W. Hwang, H. - L. Chen, C. Ting, C. - P. Chen; *Macromolecules 43* (**2010**) 3399.
12. G. Eda, G. Fanchini, M. Chhowalla; *Nature Nanotechnology* **3** (**2008**) 270.
13. M. Zhang, X. Guo, Y. Li; *Adv. Energ. Mater.* 1 (**2011**) 557.
14. W.R. Salaneck*; Physics Reports 319 (1999) 231.*
15. T. Salim, L. H. Wong, B. Bräuer, R. Kukreja, Y. L. Foo, Z. Bao, Y. M. Lam; *J. Mater. Chem. 21* (**2011**) 242.

16. A. Pivrikas, H. Neugebauer, N. S. Sariciftci; *Sol. Energ. Sol. Mat. 85* (**2011**) 1226.

17. L. Chen, Z. Hong, G. Li, Y. Yang; *Adv. Mater. 21* (**2009**) 1434.

18. R. P. Qin, W. W. Li, C. H. Li, C. Du, C. Veit, H. F. Schleiermacher, M. Andersson, Z. S. Bo, Z. P. Liu, O. Inganäs, U. Wuerfel, F. L. Zhang, *J. Am. Chem. Sol.* 131 (**2009**) 14612.

19. J. K. Lee, W. M. Li, C. J. Brabec; *J. Am. Chem. Sol. 130* (**2008**) 3619

20. X. Liu, S. Huettner, Z. Rong, M. Sommer, R. H. Friend; *Adv. Mater. 24* (**2012**) 669.

21. Y. Kim; *Nature Materials* 5 (**2006**) 197.

22. N.S. Sariciftci, "photovoltaic devices," *Materials Today, review feature,* **2007**, p. 36.

23. R. Po, M. Maggini, N. Camaioni; *J. Phys. Chem. C. 114* (**2010**) 695.

24. P. J. Brown, D. S. Thomas, A. Köhler, J. S. Wilson, J.S. Kim, C. M. Ramsdale, H. Sirringhaus, R. H. Friend, *Phys. Rev. B. 67* (**2003**) 064203.

25. Z. Tang, Master Thesis, **2010**, ISBN, ISRN: LITH-IFM-A-EX--10/2009—SE.

26. Y. Yao, J. Hou, Z. Xu, G. Li, Y. Yang; *Adv. Funct. Mater. 18* (**2008**) 1783.

27. D. Chirvase, J. Parisi, J. C. Hummelen, V. Dyakonov; *Nanotechnology. 15* (**2004**) 1317.

28. J. Rotalsky, D. Meissner; *Sol. Energy. Mater. Sol. Cells. 63* (**2000**) 37.

29. N. T. Kemp, G. U. Flanagan, A. B. Kaiser, H. J. Trodahl, B. Chapman, A. C. Partridge, R. G. Buckley; *Synth. Met. 101* (**1999**) 434.

30. S. Kivlson; *Phys. Rev. B. 25* (**1982**) 3798.

31. H. Hoppe; *J. Mater. Res. 19* (**2004**) 1924.